Formation of a Long-Lived P⁺B$_A^-$ State in Plant Pheophytin-Exchanged Reaction Centers of *Rhodobacter sphaeroides* R26 at Low Temperature[†]

John T. M. Kennis,[‡] Anatoli Ya. Shkuropatov,[§] Ivo H. M. van Stokkum,[∥] Peter Gast,[‡] Arnold J. Hoff,[‡] Vladimir A. Shuvalov,[§] and Thijs J. Aartsma[*,‡]

Department of Biophysics, Huygens Laboratory, Leiden University, P.O. Box 9504, 2300 RA, Leiden, The Netherlands, Institute of Soil Science and Photosynthesis, Russian Academy of Sciences, Pushchino, Moscow Region 142292, Russian Federation, and Faculty of Physics and Astronomy, Vrije Universiteit, De Boelelaan 1081, 1081 HV Amsterdam, The Netherlands

Received May 28, 1997; Revised Manuscript Received October 3, 1997[⊗]

ABSTRACT: Femtosecond transient absorption spectroscopy in the range of 500−1040 nm was used to study electron transfer at 5 K in reaction centers of *Rhodobacter sphaeroides* R26 in which the bacteriopheophytins (BPhe) were replaced by plant pheophytin *a* (Phe). Primary charge separation took place with a time constant of 1.6 ps, similar to that found in native RCs. Spectral changes around 1020 nm indicated the formation of reduced bacteriochlorophyll (BChl) with the same time constant, and its subsequent decay in 620 ps. This observation identifies the accessory BChl as the primary electron acceptor. No evidence was found for electron transfer to Phe, indicating that electron transfer from B$_A^-$ occurs directly to the quinone (Q$_A$) through superexchange. The results are explained by a model in which the free energy level of P⁺Phe⁻ lies above that of P⁺B$_A^-$, which itself is below P*. Assuming that the pigment exchange does not affect the energy levels of P* and P⁺B$_A^-$, our results strongly support a two-step model for primary electron transfer in the native bacterial RC, with no, or very little, admixture of superexchange.

The photosynthetic reaction center (RC)[1] is a membrane protein that converts light energy into a form of energy that is biochemically accessible to the organism. This conversion is accomplished by transferring a photoexcited electron across a membrane-spanning chain of acceptor molecules. X-ray crystallographic analysis of the RC of several purple bacteria has shown that the protein cofactors involved in electron transport are arranged in two symmetry-related branches, marked A and B (*1, 2*). It was found that electron transport exclusively takes place along the A-branch (*3*), which consists of a strongly coupled bacteriochlorophyll (BChl) dimer forming the primary electron donor P, a bacteriopheophytin (BPhe) as the primary acceptor H$_A$, and a quinone, Q$_A$. The electron is subsequently transferred to a second quinone, Q$_B$, which acquires two electrons and leaves the reaction center after protonation.

The role of the accessory BChl B$_A$, which is situated between P and H$_A$, in the charge-separation process has been debated for almost 20 years (*4−15*). No transient reduction of B$_A$ could be detected in early femtosecond measurements, which seemed to indicate that primary electron transfer occurred directly from P to H$_A$, with B$_A$ acting as a superexchange mediator (*5, 6, 8, 10, 12*). More recently, however, there is evidence that at room temperature the accessory BChl acts as a real, but short-lived intermediate in a two-step process (*13*). The extent to which electrons are transferred to H$_A$ in a two-step mechanism via B$_A$ is not clear as yet, and it was proposed that the superexchange and the two-step processes could operate in parallel (*14*). Moreover, the involvement of B$_A$ in the charge-separation process at low temperature has not yet been established.

Genetic engineering has provided a useful tool to assess the factors that govern the specific electron transfer steps (*15*). This work, however, did not unambiguously define the role of B$_A$, since mutations near P, B, or H did not modify the redox potentials of these cofactors sufficiently to result in a clear-cut transient formation of B$_A^-$. Another powerful way to modify the electron transfer properties of the RC is pigment exchange by chemical treatment. The advantage of this method is, first, that the redox potential of one specific cofactor can selectively be altered without affecting the other cofactors, and second, that a wide range of free energies can be achieved, since pigments foreign to the organism can be inserted. In this way, several RC cofactors have been exchanged for the accessory BChls, B$_{A,B}$, and the BPhes, H$_{A,B}$ (*16−20*).

Incorporation of plant pheophytin *a* (Phe) through exchange with H$_{A,B}$ brings about significant alterations of the properties of the RC. The quantum yield of quinone reduction at room temperature drops from unity in native RCs to 0.6−0.8 in plant pheophytin-exchanged RCs (*19, 21−23*). At room temperature, Shkuropatov and Shuvalov (*19*) and Schmidt et al. (*21*) detected with time-resolved spec-

troscopy an enhanced population of reduced BChl during the lifetime of Phe⁻, which was attributed to a thermal equilibrium between close-lying $P^+B_A^-$ and P^+Phe^- states. This observation strongly supported the two-step model for primary electron transfer at room temperature. According to their modeling of the kinetics, the state P^+Phe^- would lie energetically just below the state $P^+B_A^-$ (*21*), or even above that (*19*). The energetic scheme proposed by Schmidt et al. conflicts, however, with a recent study of the temperature dependence of the quantum yield of quinone reduction in plant pheophytin-exchanged RCs (*23*). This dependence could be well explained by an energy level scheme in which the free energy of P^+Phe^- lies above that of $P^+B_A^-$ (*23*).

In the present study, we report the results of a spectrally resolved femtosecond study of plant pheophytin-exchanged RCs at 5 K. We will show that the primary charge separation step involves electron transfer to the accessory BChl, and that subsequent electron transfer to the quinone occurs directly through superexchange.

EXPERIMENTAL PROCEDURES

RCs of *Rhodobacter (Rb.) sphaeroides* R26 were isolated as described in Feher and Okamura (*24*), and were modified as described in Scheer et al. (*17*), with a slight change of procedure (*19, 22*). The low-temperature absorption spectrum of the preparation used (not shown) was similar to that published earlier (*22*). There was still some residual absorption at 760 nm, which indicates that not all $H_{A,B}$ pigments had been exchanged for Phe. Comparison with the absorption spectrum of native RCs from *Rb. sphaeroides* R26 indicated an exchange yield of 88%. Because there is evidence that H-exchange preferentially takes place on the inactive B-branch (*22*), we conclude that in our preparation close to 25% of the RCs still have a BPhe molecule in its A branch. This fraction of RCs, denoted as H_B-only exchanged RCs, is expected to perform normal photochemistry (*22, 23*).

The samples were mixed with glycerol (65% v/v) to obtain a clear glass at low temperature, transferred to a 1 mm cuvette, and then cooled in the dark to 5 K in a helium flow cryostat (Utreks, Estonia). The low-temperature absorption of the samples was adjusted to either 1.0 at 800 nm or 1.0 at 890 nm.

Femtosecond transient absorption measurements were carried out with a home-built amplified dye laser system with continuum generation and optical multichannel analyzer (OMA) detection, described in Kennis et al. (*25*) with some modifications (*26*), operating at 10 Hz. Excitation pulses centered at 900 nm, with a spectral width of about 50 nm, were obtained by amplifying part of the continuum in a glass flow cuvette filled with a solution of the dye LDS 867 (Exciton) in propylene carbonate. Wavelengths shorter than 850 nm in the pump beam were cut off with an RG850 filter (Melles Griot). The intensity was adjusted to provide a maximum bleaching of 10−20% of the P-band. Pump and probe pulses were polarized parallel to each other. The overlap of pump and probe pulses was verified by visual inspection using a video camera attached to a simple microscope.

For measurements with the plant pheophytin-exchanged RCs, 4 sets of 32 time-resolved spectra were taken spanning

a time interval of 1.5 ns, each set having a width of 155 nm. The spectra overlapped one another at the edges of the wavelength range and were connected to cover the spectral region from 650 nm to 1040 nm. In the Q_x region of $H_{A,B}$ and Phe, i.e., around 545 nm, six time-resolved spectra were taken.

For native RCs, 35 time-resolved spectra in the spectral range from 880 nm to 1040 nm were taken in a time interval of 1.5 ns. In the Q_x region of $H_{A,B}$, six spectra at various delays were taken.

Group velocity dispersion in the white-light continuum was taken into account by recording the transient birefringence in CS_2 (*27*), and the time-resolved spectra presented in Figure 1A were corrected accordingly. The time-resolved spectra presented in Figure 1B were taken at sufficiently long delay to ignore effects of group velocity dispersion.

Global analysis was applied to the data according to a procedure described earlier (*28*). The instrument response function was described by a Gaussian with a full width at half-maximum of 650 fs. Time-zero of the instrument response was described by a third-order polynomial of the wavelength to take into account group velocity dispersion. This polynomial function was independently checked with the dispersion measurement in CS_2.

RESULTS AND INTERPRETATION

Time-Resolved Spectra. Figure 1 shows time-resolved spectra over the red and near-infrared region upon excitation at 900 nm in Phe-exchanged RCs at 5 K. At a delay of 0.5 ps (Figure 1A, dashed line), a broad bleaching near 890 nm with a shoulder near 930 nm is observed, which we attribute to ground-state depletion and to stimulated emission from the excited primary donor, respectively. Small band shifts are observed around 800 and 670 nm. They reflect the response of $B_{A,B}$ and $Phe_{A,B}$ to excitation of the primary donor, similar to the situation in native RCs (*15, 29*).

In the course of a few picoseconds, the stimulated emission disappears. The right inset of Figure 1A highlights the spectral region around 1020 nm. A pronounced absorbance increase is observed at 1020 nm, which rises concomitantly with the disappearance of stimulated emission. Reduced BChl *a in vitro* has a small absorption band at 1000 nm (*30*), which appears to shift to 1020 nm *in vivo* (*13*). The observation of this band in the transient spectra shown in Figure 1 gives direct evidence that the primary charge-separation step at 5 K involves electron transfer to the accessory BChl. At room temperature, low-resolution, weak absorbance changes near 1020 nm have been observed by Zinth and co-workers in native RCs, plant pheophytin-exchanged RCs, and 3-vinyl bacteriopheophytin-exchanged RCs (*13, 20, 21*), and have also been taken as evidence for the transient formation of B_A^-.

At 10 ps delay (solid line), the stimulated emission from the primary donor has largely disappeared, and a bleaching has developed around 800 nm accompanied by a small absorbance increase near 780 nm. This asymmetry means that the change at 800 nm is not purely an electrochromic band shift as in native RCs (*3, 15*), and is another indication that electron transfer to B_A takes place. Around 675 nm, where the newly incorporated Phe molecules absorb, an absorbance decrease is observed with a symmetric absorbance increase at either side of the band. Experiments by
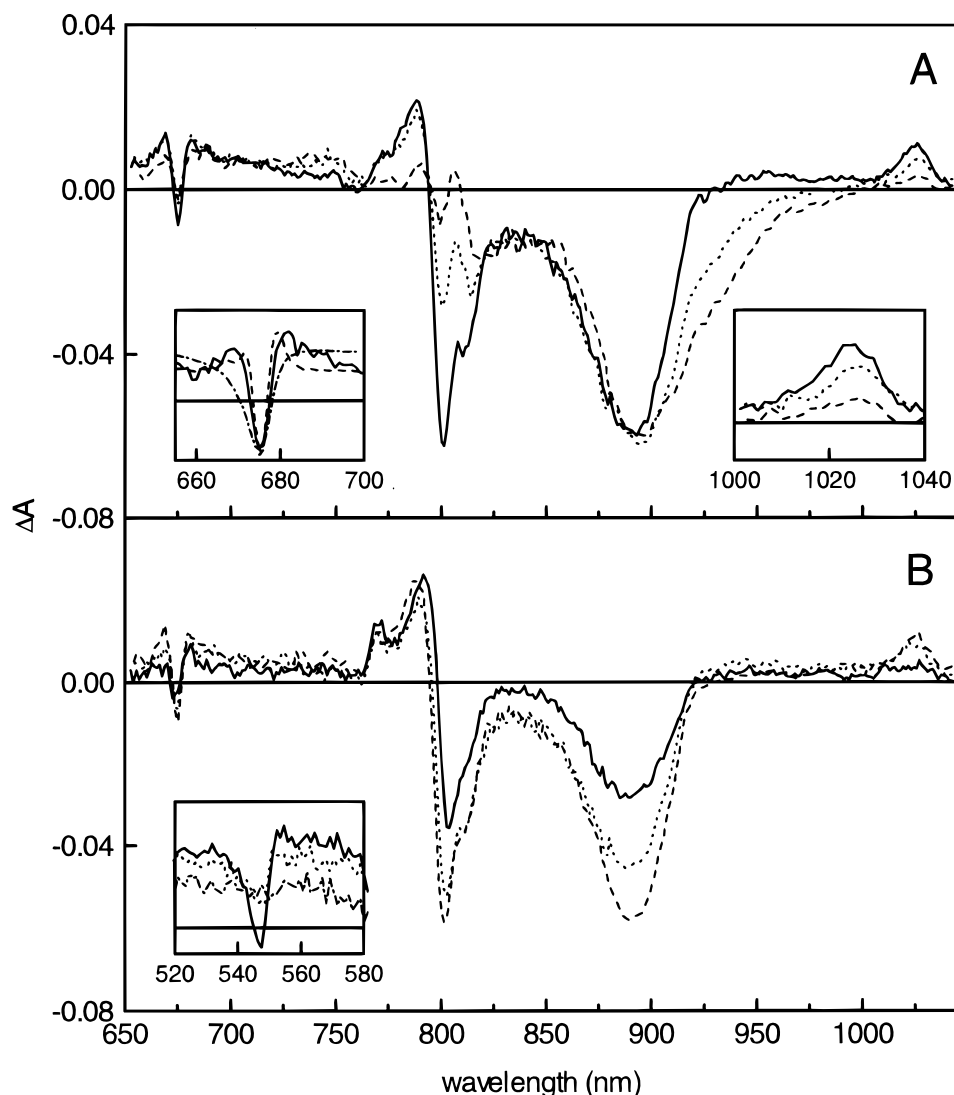
FIGURE 1: (A) Time-resolved spectra in plant pheophytin-exchanged RCs upon excitation at 900 nm at 5 K at delays of 0.5 ps (dashed line), 1.5 ps (dotted line), and 10 ps (solid line). The right inset shows the spectral region around 1020 nm, with time-resolved spectra at 0.5 ps (dashed line), 1.5 ps (dotted line), and 7.5 ps (solid line). The left inset shows the spectral region around 670 nm, with the difference spectrum at a delay of 120 ps (solid line), the inverted second derivative of the absorption spectrum of the sample offset by 0.005 (dashed line), and the inverted absorption spectrum of the sample offset by 0.006 (dash−dotted line). (B) Time-resolved spectra at delays of 60 ps (dashed line), 240 ps (dotted line), and 1.2 ns (solid line). The inset shows the spectral region around 550 nm, with the difference spectrum at delays of 12 ps (solid line), 100 ps (dotted line), and 1 ns (dash−dotted line).

Franken et al. (23) indicate that electron transfer from P* to Phe does not occur in pheophytin-exchanged RCs at low temperature. Therefore, it seems unlikely that this signal represents ground-state bleaching of Phe. Actually, the width of the bleaching (5 nm) is smaller than the width of the Phe band in the absorption spectrum. The shape of the signal resembles the second derivative of the 675 nm absorption band, which suggests that it is a symmetric double-band shift or a line broadening. The second-derivative signal around 675 nm is formed with the same time constant and has the same lifetime as the absorbance increase at 1020 nm (see below), which is a strong indication that it is associated with the state $P^+B_A^-$. The signal is shown in more detail in the left inset of Figure 1A, where the time-resolved signal around 675 nm at a delay of 120 ps is shown (solid line), together with the Phe absorption band (dash−dotted line) and its second derivative (dashed line). The occurrence of a second-derivative signal is remarkable, because in oriented samples the linear Stark effect is expected to produce first-derivative signals only. The broadening may be associated with a

different electric field effect on Phe_A and Phe_B by the state $P^+B_A^-$. Additional experiments are needed to clarify this issue. Based on these considerations, we assume that in pheophytin-exchanged RCs no electron transfer to Phe takes place, and conclude that the time-resolved spectrum at 10 ps delay is largely due to the radical pair $P^+B_A^-$. However, the spectrum at 10 ps will also contain a contribution from the 25% fraction of H_B-only exchanged RCs, which will mainly be in the state $P^+H_A^-$. The H_B-only exchanged RCs manifest themselves most distinctly by the bleaching at 760 nm (Figure 1A) and 547 nm (Figure 1B, inset), where the Q_y and Q_x bands of H_A are located. Because Phe appears not to be reduced in $H_{A,B}$-exchanged RCs, we assign the signal at 547 nm entirely to the state $P^+H_A^-$ in H_B-only exchanged RCs.

Figure 1B shows the time-resolved spectra at longer delays. At 60 ps (dashed line) and 240 ps delay (dotted line), the bands at 1020, 800, and 670 nm have not changed much, whereas the band at 547 nm has decreased significantly after 100 ps. These observations show, first, that the decay of
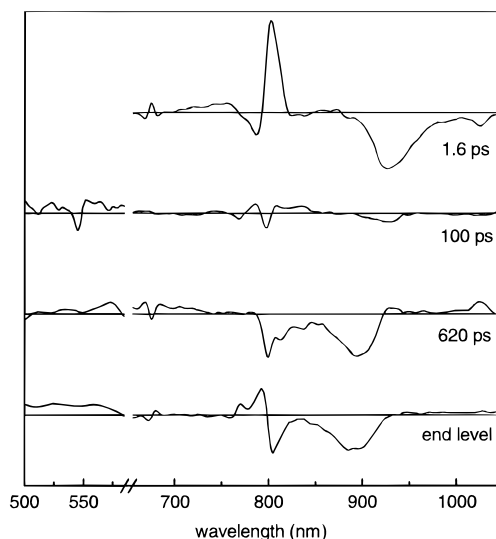
FIGURE 2: Decay-associated difference spectra (DADS) that result from global analysis of the time-resolved spectra of plant pheophytin-exchanged RCs of *Rhodobacter sphaeroides* R26 upon excitation at 900 nm at 5 K. From top to bottom, the spectra are shown that are associated with the 1.6 ps component, the 100 ps component, the 620 ps component, and the irreversible end level, respectively. The spectra in the region of 500−580 nm are enlarged 5 times with respect to the spectra in the region from 650 to 1040 nm.

the 547 nm band results from electron transfer from H_A to Q_A in the fraction of H_B-only exchanged RCs, which transfer typically occurs with a time constant of 100 ps (*3*), and second, that the lifetime of the $P^+B_A^-$ radical pair in $H_{A,B}$-exchanged RCs is several hundreds of picoseconds.

At a delay of 1.2 ns (solid line), the 1020 nm band, the net bleaching at 800 nm, and the line-broadening signal at 670 nm have diminished considerably, indicating decay of the $P^+B_A^-$ radical pair. The difference spectrum at 1.2 ns very much resembles the state $P^+Q_A^-$ as measured previously in $H_{A,B}$-exchanged and H_B-only exchanged RCs (*22, 31*), with a bleaching of P, a major band shift of B_A and/or B_B, and a minor band shift of Phe. The absorption increase at 770 nm is due to H_A in H_B-only exchanged RCs. The bleaching of P at 890 nm has decreased by a about a factor of 2 with respect to its value at a delay of 10 ps, which implies that the total quantum yield of $P^+Q_A^-$ formation is 0.5. This number is consistent with the known quantum yield in $H_{A,B}$-exchanged RCs (0.38) (*23*), and the presence of 25% H_B-only exchanged RCs in the preparation, which have a quantum yield of $P^+Q_A^-$ formation of unity (i.e., $0.25 \times 1 + 0.75 \times 0.38 = 0.5$).

Global Analysis of the Time-Resolved Spectra. To find the rate constants and spectra for the formation and decay of the excited and radical-pair states involved, we have applied a global analysis to the time-resolved spectra, a few of which are shown in Figure 1. When analyzing the data as a sum of exponentials, three time constants of 1.6, 100, and 620 ps and an irreversible end level are needed to describe the data. The corresponding decay-associated difference spectra (DADS) are plotted in Figure 2. The root mean square error of the fit was 1.5×10^{-3} units of absorbance.

The 1.6 ps difference spectrum represents decay of stimulated emission from P near 930 nm and formation of the BChl anion absorbance increase at 1020 nm, the
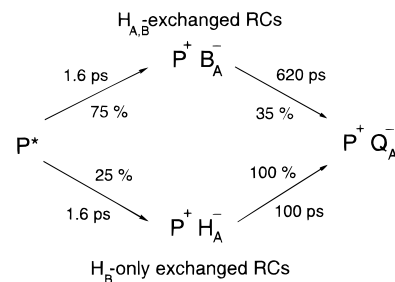

FIGURE 3: Kinetic scheme to account for the two parallel pathways of electron transfer in the fractions of $H_{A,B}$-exchanged RCs and H_B-only exchanged RCs. See text for details.

bleaching of B at 800 nm, and the Phe line broadening at 675 nm, all associated with the difference spectrum of B_A^- as assigned above. Especially the observation that the $BChl^-$ anion band at 1020 nm rises concomitantly with the decay of stimulated emission from P* proves that primary charge separation in the $H_{A,B}$-exchanged RCs occurs in 1.6 ps. The signals of the H_B-only exchanged RCs contribute also to the 1.6 ps difference spectrum, but they will have no intensity in the 1020 nm region. Charge separation in these RCs presumably occurs with the same time constant as in native RCs, which occurs with an average time constant of 1.8 ps (see below), and thus is essentially the same as in the fully exchanged RCs.

The 100 ps DADS spectrum is due to electron transfer from H_A to Q_A in the fraction of H_B-only exchanged RCs, and involves only minor spectral changes in the Q_y region, as seen previously (*3*): a bleaching of the H_A band at 760 nm, a slight red shift of the electrochromic band shift around 800 nm, and the appearance of a small absorption increase near 770 nm. The spectrum accounts for all the decay in the 550 nm region, in accordance with the assumption that this signal is solely due to the fraction of H_B-only exchanged RCs. It also shows some intensity in the region of stimulated emission of P, which may be indicative of some heterogeneity in the primary charge-separation kinetics (*32−34*).

The DADS with a lifetime of 620 ps represents decay of the state $P^+B_A^-$. It shows a bleaching of P at 890 nm, a bleaching of B_A at 800 nm, an absorbance increase at 1020 nm, a broad absorbance increase near 670 nm, and the line-broadened signal of Phe at 675 nm, signals which are associated with recombination of the state $P^+B_A^-$ to the ground state and with the spectral changes corresponding to electron transfer to Q_A.

The long-lived end level is virtually identical to the spectrum at 1.2 ns in Figure 1B, and represents the state $P^+Q_A^-$ in $H_{A,B}$-exchanged and the fraction of H_B-only exchanged RCs.

A description of the data as a sum of exponentials yields the time constants for the electron transfer processes in the $H_{A,B}$-exchanged/H_B-only exchanged RC mixture, but it does not result in the spectrum of the pure $P^+B_A^-$ state, the determination of which is one of the goals of this study. To this end, we have analyzed the data using the parallel scheme of Figure 3. We assume that the state P* is spectrally and kinetically indistinguishable in $H_{A,B}$-exchanged and H_B-only exchanged RCs. On the basis of the steady-state absorption spectrum of the sample, we assume as before that 75% of the RCs is $H_{A,B}$-exchanged, and 25% H_B-only exchanged (see Experimental Procedures). Furthermore, we assume that the yield of electron transfer from B_A to Q_A in $H_{A,B}$-exchanged
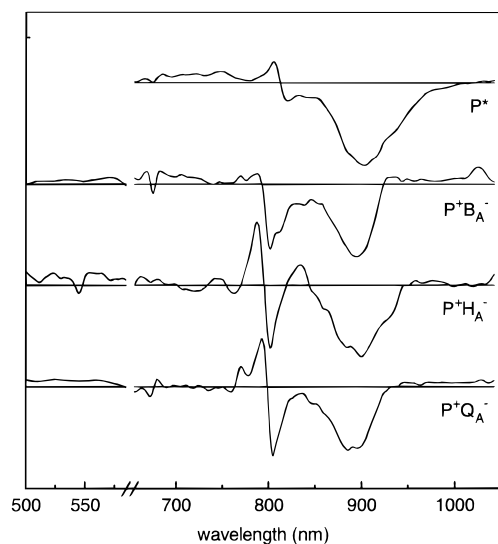
FIGURE 4: Species-associated difference spectra (SADS) that follow from global analysis of the time-resolved spectra of plant pheophytin-exchanged RCs of *Rhodobacter sphaeroides* R26 upon excitation at 900 nm at 5 K in terms of the parallel scheme depicted in Figure 3. From top to bottom, the spectra represent the states P*, $P^+B_A^-$, $P^+H_A^-$, and $P^+Q_A^-$, respectively.

RCs is equal to 0.38 (*23*). Note that it is not possible to distinguish the two types of $P^+Q_A^-$ difference spectra in the spectra at long delay times (>1 ns). However, the difference spectrum of the state $P^+Q_A^-$ is expected to be the same in $H_{A,B}$-exchanged and H_B-only exchanged RCs, apart from a positive feature around 770 nm (*22*). The time constants of the various electron transfer steps were fixed at 1.6, 100, and 620 ps, as indicated in Figure 3.

The species-associated difference spectra (SADS) that result from the above analysis are shown in Figure 4. The difference spectrum associated with P* is very similar to that published for native RCs at low temperature (*15, 29*). The spectrum associated with the state $P^+H_A^-$ in the fraction of H_B-only exchanged RCs, though somewhat noisy (due to the relatively small contribution that the H_B-only exchanged RCs make to the total signal), much resembles the corresponding spectrum from the literature recorded for native RCs, with a bleaching of P near 890 nm and an electrochromic band shift of the accessory BChls around 800 nm (*3, 15, 29*). As expected, the spectrum also shows a bleaching of the Q_x band of H_A at 547 nm. The $P^+B_A^-$ difference spectrum exhibits, apart from the bleaching of the primary donor, an absorption increase at 1020 nm, a bleaching at 800 nm, a small absorbance increase around 790 nm, and a broad absorbance increase near 670 nm, all in accordance with the *in vitro* BChl/BChl$^-$ difference spectrum at room temperature reported by Fajer et al. (*30*). Superimposed on the broad absorbance increase, we find the line-broadened signal of Phe at 675 nm (see Figure 1A). The ratio between the bleaching near 800 nm and the absorbance increase near 1020 nm is the same as in the BChl$^-$ difference spectrum (*30*), which supports our idea that this difference spectrum purely represents the state $P^+B_A^-$. The $P^+B_A^-$ difference spectrum also resembles the corresponding room-temperature difference spectrum that Holzwarth and Müller (*35*) have extracted from their time-resolved difference spectra recorded for *Rb. sphaeroides* wild-type RCs.

Comparison with Native RCs. To investigate the extent to which B_A is populated in the native bacterial RC at low
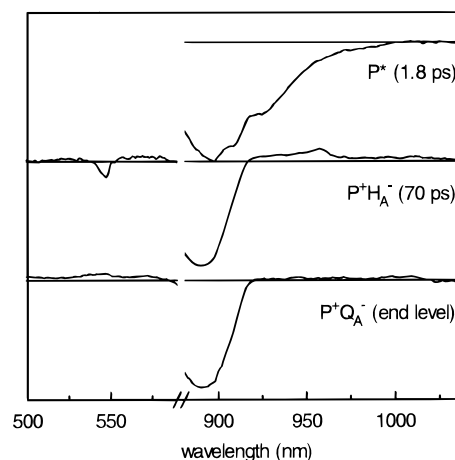

FIGURE 5: Species-associated difference spectra (SADS) that result from global analysis of time-resolved spectra of native RCs of *Rhodobacter sphaeroides* R26 upon excitation at 900 nm at 5 K, with, from top to bottom, spectra associated with P* (1.8 ps component), $P^+H_A^-$ (70 ps component), and $P^+Q_A^-$ (irreversible end level), respectively.

temperature, we performed time-resolved measurements on native *Rb. sphaeroides* R26 RCs in the 880−1040 and 550 nm regions at 5 K. Global analysis showed that two time constants of 1.8 and 70 ps and a long-lived end level are required to adequately describe the data. Figure 5 shows the resulting SADS. The 1.8 ps component represents the state P*, which shows ground-state bleaching and stimulated emission of P. Primary charge separation in these native RCs at 5 K thus occurs with a time constant of 1.8 ps. This value appears to be somewhat longer than those reported earlier, which vary between 1.2 ps (*8*) and 1.4 ps (*36*). According to Vos et al., primary charge separation at 10 K is biexponential with time constants of 0.9 ps (80%) and 4.5 ps (20%) (*37*). The signal-to-noise of our measurements is not sufficient to resolve biexponential decays, but the weighted average time constant of the decays found by Vos et al., 1.6 ps, agrees well with our value of 1.8 ps. We furthermore note that our analysis is based on the dynamics of the entire stimulated emission band, whereas all previous reports based their values on decay of the stimulated emission at a single wavelength. In this respect, it is interesting to note that a full spectral analysis of *Rb. capsulatus* wild-type RCs at 20 K revealed a major time constant of decay of stimulated emission of 1.3 ps and a minor one of 6 ps, which were spectrally shifted with respect to each other (*38*). This indicates that the rate of decay of stimulated emission, when monitored single-wavelength, may be dependent on the detection wavelength. A similar dependence on detection wavelength, although only qualitatively analyzed, was observed in *Rb. sphaeroides* R26 RCs at low temperature (*29*).

The SADS with a lifetime of 70 ps shows ground-state bleaching of the primary donor and the appearance of a small absorbance increase at 958 nm. It also shows a bleaching of the Q_x band of H_A at 547 nm, which indicates that it is associated with the state $P^+H_A^-$. The time constant for electron transfer from H_A to Q_A, 70 ps, agrees reasonably well with the values reported earlier (*3*). The spectrum of the long-lived component only shows ground-state bleaching of the primary donor and a broad absorbance increase at longer wavelengths, and may be assigned to the state $P^+Q_A^-$.

We do not find clear evidence for a BChl anion band at 1020 nm. However, when introducing an extra component

with a fixed time of 0.3 ps after the 1.8 ps component (*36*), its SADS possessed an absorbance increase centered at 1020 nm (results not shown). Thus, although our data do not provide independent evidence, they are consistent with the presence of $P^+B_A^-$ as an intermediate that is at the detection limit of our apparatus.

The 958 nm band in the SADS of the 70 ps component is due to the reduction of H_A. It is similar to the one observed in the H_A^- photoaccumulation difference spectrum of LH1−RC complexes of *Chromatium minutissimum* (*39*) and in RCs of *Rb. sphaeroides* R26 (*40*). It can also be observed in the time-resolved spectra at 10 K in wild-type RCs of *Rb. sphaeroides* by Vos et al. (*41*) and in the room-temperature DADS by Arlt et al. (*13*) in *Rb. sphaeroides* R26 RCs. These authors do not assign the 958 nm band, but rather attribute the entire broad, featureless absorbance increase at wavelengths beyond 920 nm to the presence of P^+. However, Vos et al. (*41*) did not record spectra at delays longer than 100 ps, which implies that a significant part of the RCs was still in the state $P^+H_A^-$. In the DADS by Arlt et al. (*13*), the 958 nm band showed up in the 200 ps component, which supports our conclusion that it is associated with reduction of H_A. In principle, the 958 nm band should also be observed in the fraction of H_B-only exchanged RCs in the time-resolved spectra of Figure 1A, but given the noise in these spectra it was too small to be detected. We note that the *in vitro* difference spectrum of reduced BPhe shows a positive absorption band at 880 nm (*30*). Most probably, this band has shifted to 958 nm in the RC, perhaps associated with the presence of the glutamic acid at position L104, which is hydrogen-bonded to H_A (*42*).

DISCUSSION

Electron Transfer in Plant Pheophytin-Exchanged RCs. In a recent publication, Franken et al. report the results of a careful study of the quantum yield of $P^+Q_A^-$ formation as a function of temperature in pheophytin-exchanged RCs (*23*). These measurements showed that the $P^+Q_A^-$ yield drops from 75% at room temperature to 38% at 10 K. The temperature dependence of the quantum yield could be accounted for quantitatively by the assumption that the P^+Phe^- state is higher in energy (by about 210 cm^{-1}) than the $P^+B_A^-$ state. This implies that Phe is not reduced in the exchanged RCs at temperatures of 5 K, as in the present experiments. The conclusion concerning the relative energies of the P^+Phe^- and $P^+B_A^-$ states is consistent with the reduced yield of triplet state formation, which was at least an order of magnitude lower than in native RCs (*23*). Apparently, the radical-pair mechanism (*43*) is not operative, indicating that the P^+Phe^- state is not formed. Because of strong coupling, triplet state formation from the $P^+B_A^-$ state has a much lower probability than from the $P^+H_A^-$ state. Moreover, the recombination lifetime of $P^+B_A^-$ in pheophytin-exchanged RCs (1 ns, see below) is much shorter than that of $P^+H_A^-$ in native RCs (20 ns) (*23*). Based on these observations, Franken et al. (*23*) proposed an energy level diagram which is reproduced in Figure 6.

Our low-temperature time-resolved measurements on plant pheophytin-exchanged RCs of *Rb. sphaeroides* R26 are in full agreement with the model proposed by Franken et al. (*23*). The time-resolved experiments clearly show that the primary charge-separation step involves electron transfer
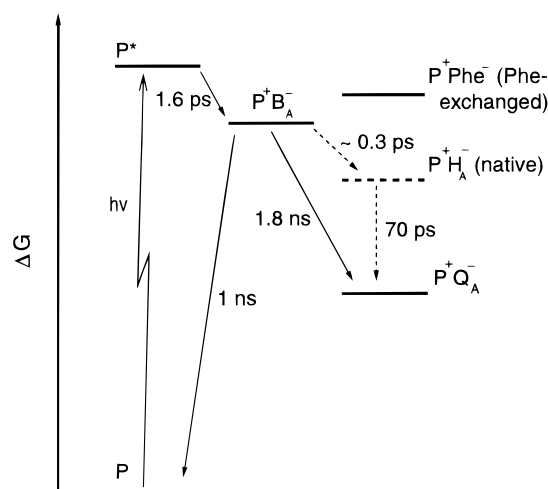

FIGURE 6: Energy level scheme of plant pheophytin-exchanged and native RCs. The dashed arrows denote the electron transfer steps in native RCs after electron transfer from P* to B_A. The value of 0.3 ps in the native RC for electron transfer from B_A to H_A is taken from ref 36.

from P* to the accessory BChl, and that the radical-pair state $P^+B_A^-$ has a lifetime of 620 ps at 5 K. These observations prove that the free energy level of $P^+B_A^-$ lies lower than that of P*, at least at 5 K. There is no evidence that Phe is reduced, which either means that P^+Phe^- lies above $P^+B_A^-$, similar to the conclusions by Shkuropatov and Shuvalov (*19*) and Franken et al. (*23*), or that there is an energy barrier between $P^+B_A^-$ and P^+Phe^-. The latter possibility would correspond to a two-step model for electron transfer from B_A to Q_A, with the state P^+Phe^- as a short-lived intermediate. However, such a model would be incompatible with the quantum yield of ^3P formation in prereduced RCs at low temperature, as argued by Franken et al. (*23*), and is therefore dismissed.

Considering the low temperature at which our measurements were performed, and according to the scheme of Figure 6, electron transfer to Q_A cannot take place via Phe. However, electron transfer can proceed directly from B_A to Q_A with Phe as a superexchange mediator (*23, 44, 45*). For the primary charge-separation, we find a rate of (1.6 ps)$^{-1}$, very much like that of native RCs. Given the quantum yield for Q_A reduction of 0.38 (*23*) and a lifetime of 620 ps for the state $P^+B_A^-$, we find that the electron transfer rate to the quinone equals (1.8 ns)$^{-1}$, and the recombination rate to the ground state equals (1 ns)$^{-1}$.

Schmidt et al. (*21*) have explained the results of their room-temperature femtosecond measurements on plant pheophytin-exchanged RCs by putting the level of P^+Phe^- slightly below $P^+B_A^-$. This arrangement conflicts, however, with the present low-temperature results and the results of Franken et al. (*23*), as stated above. The choice of the relative free energies for P^+Phe^- and $P^+B_A^-$ of Schmidt et al. was mostly based on the relative concentrations of the states $P^+B_A^-$ and P^+Phe^- after primary charge separation. The determination of these concentrations relied on a comparison of absolute cross sections of the 1020 nm BChl anion band *in vitro* and in the RC. We believe that this is an inherently difficult and unreliable procedure that easily may have led to an underestimation of the concentration of $P^+B_A^-$ with respect to P^+Phe^-.

The charge-separation characteristics in plant pheophytin-exchanged RCs are strikingly similar to those in mutant RCs

of *Rb. sphaeroides* where leucine at position 214 at the M-subunit has been replaced by histidine, resulting in replacement of H_A by a BChl (denoted as β). In these β-type RCs, primary charge separation takes place with a time constant of 2.6 ps at 5 K, and the resulting radical pair lives for 800 ps, while the quantum yield for quinone reduction is 0.25 (*44, 45*). At room temperature, these numbers are 5.8 ps, 350 ps, and 0.6, respectively, similar to the corresponding numbers found for plant pheophytin-exchanged RCs by Shkuropatov and Shuvalov (*19*) and Schmidt et al. (*21*). Although in the β-type RCs it is impossible to spectrally distinguish B_A from β, it was suggested on the basis of the kinetic behavior of the charge-separated states that the population of the state $P^+B_A^-$ would dominate over $P^+\beta^-$ (*44*). Given the similarity with the results presented here, it indeed seems likely that the free energy level of the state $P^+\beta^-$ lies above that of $P^+B_A^-$ in β-type RCs.

It was estimated that the $P^+B_A^-$ level lies ca. 70 meV below P* (*21, 44−46*), and that $P^+H_A^-$ lies 150−250 meV below P* (*47−51*). The difference in midpoint potential between BPhe and Phe *in vitro* is 160 meV (*20*). According to these numbers, the P^+Phe^- level should lie in the vicinity of $P^+B_A^-$, and given the scatter in the reported values for the radical-pair free energy levels, these data are consistent with our finding that P^+Phe^- lies above $P^+B_A^-$.

Involvement of B_A in Primary Charge Separation in Native RCs at 5 K. It is reasonable to assume that the pigment exchange only affects the energy level of $P^+H_{A,B}^-$, from which it follows that in native RCs, the free energy level of $P^+B_A^-$ lies below P* as well. This observation does not necessarily imply that electron transfer is purely a two-step mechanism; i.e., superexchange then may still contribute to the overall electron transfer process (*14, 52*). If a two-step mechanism and superexchange pathway would operate in parallel in the electron transfer from P* to H_A, a shutdown of the superexchange pathway, as in pheophytin-exchanged RCs, would result in a decrease of the rate of primary charge separation. However, the rate of charge separation for plant pheophytin-exchanged RCs is essentially the same as for native RCs, at 5 K as is demonstrated in this work, and at room temperature (*21*). This indicates that electron transfer in native RCs is a two-step process in which the electron is transferred to B_A prior to H_A, and that the electron transfer rate from B_A^- to H_A is much faster than from P* to B_A, as proposed by Zinth and co-workers (*9, 13*). We thus conclude that the superexchange pathway provides, if any, only a minor contribution to the primary charge-separation process in the bacterial RC. There is, however, a clear need for low-temperature measurements in the B_A^- region near 1020 nm with higher sensitivity and better time resolution than in the present study to determine the rate of electron transfer from B_A to H_A at low temperature.

ACKNOWLEDGMENT

REFERENCES

1. Deisenhofer, J., Epp, O., Miki, K., Huber, R., and Michel, H. (1984) *J. Mol. Biol. 180*, 385.
2. Allen, J. P., Feher, G., Yeates, T. O., Komiya, H., and Rees, D. C. (1987) *Proc. Natl. Acad. Sci. U.S.A. 84*, 5730.
3. Kirmaier, C., Holten, D., and Parson, W. W. (1985) *Biochim. Biophys. Acta 810*, 49.
4. Shuvalov, V. A., Klevanik, A. V., Sharkov, A. V., Matveetz, Ya. A., and Krukov, P. G. (1978) *FEBS Lett. 91*, 135.
5. Martin, J.-L., Breton, J., Hoff, A. J., Migus, A., and Antonetti, A. (1986) *Proc. Natl. Acad. Sci. U.S.A. 83*, 957.
6. Breton, J., Martin, J.-L., Migus, A., Antonetti, A., and Orszag, A. (1986) *Proc. Natl. Acad. Sci. U.S.A. 83*, 5121.
7. Chekalin, S. V., Matveetz, Ya. A., Shkuropatov, A. Ya., Shuvalov, V. A., and Yartzev, A. P. (1987) *FEBS Lett. 216*, 245.
8. Breton, J., Martin, J.-L., Fleming, G. R., and Lambry, J.-C. (1988) *Biochemistry 27*, 8276.
9. Holzapfel, W., Finkele, U., Kaiser, W., Oesterheld, D., Scheer, H., Stilz, H. U., and Zinth, W. (1989) *Chem. Phys. Lett. 160*, 1.
10. Kirmaier, C., and Holten, D. (1990) *Proc. Natl. Acad. Sci. U.S.A. 87*, 3552.
11. Dressler, K., Umlauf, E., Schmidt, S., Hamm, P., Zinth, W., Buchanan, S., and Michel, H. (1991) *Chem. Phys. Lett. 183*, 270.
12. Kirmaier, C., and Holten, D. (1991) *Biochemistry 30*, 609.
13. Arlt, T., Schmidt, S., Kaiser, W., Lauterwasser, C., Meyer, M., Scheer, H., and Zinth, W. (1993) *Proc. Natl. Acad. Sci. U.S.A. 90*, 11757. Van Stokkum, I. H. M., Beekman, L. M. P., Jones, M. R., Van Brederode, M. E., and Van Grondelle, R. (1997) *Biochemistry 36*, 11360.
14. Bixon, M., Jortner, J., and Michel-Beyerle, M. E. (1991) *Biochim. Biophys. Acta 1056*, 301.
15. Woodbury, N. W., and Allen, J. P. (1995) in *Anoxygenic Photosynthetic Bacteria* (Blankenship, R. E., Madigan, M. T., and Bauer, C. E., Eds.) p 527, Kluwer Academic Publishers, Dordrecht, The Netherlands.
16. Struck, A., Beese, D., Cmiel, E., Fischer, M., Muller, A., Schafer, W., and Scheer, H. (1990) in *Springer Series in Biophysics, Vol 6. Reaction Centers of Photosynthetic Bacteria* (Michel-Beyerle, M. E., Ed.) p 313, Springer, Berlin.
17. Scheer, H., Meyer, M., and Katheder, I. (1992) in *The Photosynthetic Bacterial Reaction Center II: Structure, Spectroscopy and Dynamics* (Breton, J., and Verméglio, A., Eds.) *NATO ASI Ser. A: Life Sci. 237*, 49, Plenum Press, New York.
18. Finkele, U., Lauterwasser, C., Struck, A., Scheer, H., and Zinth, W. (1992) *Proc. Natl. Acad. Sci. U.S.A. 89*, 9512.
19. Shkuropatov, A. Ya., and Shuvalov, V. A. (1993) *FEBS Lett. 322*, 168.
20. Huber, H., Meyer, M., Nägele, T., Hartl, I., Scheer, H., Zinth, W., and Wachtveitl, J. (1995) *Chem. Phys. Lett. 197*, 297.
21. Schmidt, S., Arlt, T., Hamm, P., Huber, H., Nägele, T., Wachtveitl, J., Meyer, M., Scheer, H., and Zinth, W. (1994) *Chem. Phys. Lett. 223*, 116.
22. Franken, E. M., Shkuropatov, A. Ya., Francke, C., Neerken, S., Gast, P., Shuvalov, V. A., Hoff, A. J., and Aartsma, T. J. (1997) *Biochim. Biophys. Acta 1319*, 242.
23. Franken, E. M., Shkuropatov, A. Ya., Francke, C., Neerken, S., Gast, P., Shuvalov, V. A., Hoff, A. J., and Aartsma, T. J. (1997) *Biochim. Biophys. Acta 1321*, 1.
24. Feher, G., and Okamura, M. Y. (1978) in *The Photosynthetic Bacteria* (Clayton, R. K., and Sistrom, W. R., Eds.) p 349, Plenum Press, New York.
25. Kennis, J. T. M., Streltsov, A. M., Aartsma, T. J., Nozawa, T., and Amesz, J. (1996) *J. Phys. Chem. 100*, 2438.
26. Kennis, J. T. M., Streltsov, A. M., Permentier, H., Aartsma, T. J., and Amesz, J. *J. Phys. Chem.* (in press).
27. Greene, B. J., and Farrow, R. C. (1983) *Chem. Phys. Lett. 98*, 273.
28. van Stokkum, I. H. M., Brouwer, A. M., Van Ramesdonk, H. J., and Scherer, T. (1990) *Proc. K. Ned. Akad. Wet. 96*, 43.
29. Peloquin, J. M., Lin, S., Taguchi, A. K. W., and Woodbury, N. W. (1996) *J. Phys. Chem 100*, 14228.

30. Fajer, J., Brune, D. C., Davis, S., Forman, A., and Spaulding, L. D. (1975) *Proc. Natl. Acad. Sci. U.S.A. 72*, 4956.

31. Shkuropatov, A. Ya., Proskuryakov, I. I., Shkuropatova, V. A., Zvereva, M. G., and Shuvalov, V. A. (1994) *FEBS Lett. 351*, 249.

32. Du, M., Rosenthal, S. J., Xie, X., DiMagno, J., Schmidt, M., Hanson, D. K., Schiffer, M., Norris, J. R., and Fleming, G. R. (1992) *Proc. Natl. Acad. Sci. U.S.A. 89*, 8517.

33. Müller, M. G., Griebenow, K., and Holzwarth, A. R. (1992) *Chem. Phys. Lett. 199*, 465.

34. Beekman, L. M. P., Van Stokkum, I. H. M., Monshouwer, R., Rijnders, A. J., McGlynn, P., Visschers, R. W., Jones, M. R., and Van Grondelle, R. (1996) *J. Phys. Chem. 100*, 7256.

35. Holzwarth, A. R., and Müller, M. G. (1996) *Biochemistry 35*, 11820.

36. Lauterwasser, C., Finkele, U., Scheer, H., and Zinth, W. (1991) *Chem. Phys. Lett. 183*, 471.

37. Vos, M. H., Lambry, J.-C., Robles, S. J., Youvan, D. C., Breton, J., and Martin, J.-L. (1992) *Proc. Natl. Acad. Sci. U.S.A. 89*, 613.

38. Lin, S., Xiao, W., Eastman, E., Taguchi, A. K. W., and Woodbury, N. W. (1996) *Biochemistry 35*, 3187.

39. Shuvalov, V. A., and Klimov, V. V. (1976) *Biochim. Biophys. Acta 440*, 587.

40. Okamura, M. Y., Isaacson, R. A., and Feher, G. (1979) *Biochim. Biophys. Acta 546*, 394.

41. Vos, M. H., Jones, M. R., Hunter, C. N., Breton, J., Lambry, J.-C., and Martin, J.-L. (1994) *Biochemistry 33*, 6750.

42. Bylina, E. J., Kirmaier, C., McDowell, L., Holten, D., and Youvan, D. C. (1988) *Nature 336*, 182.

43. Budil, D. E., and Thurnauer, M. C. (1991) *Biochim. Biophys. Acta 1057*, 1.

44. Kirmaier, C., Laporte, L., Schenck, C. C., and Holten, D. (1995) *J. Phys. Chem. 99*, 8903.

45. Kirmaier, C., Laporte, L., Schenck, C. C., and Holten, D. (1995) *J. Phys. Chem. 99*, 8910.

46. Shuvalov, V. A., and Parson, W. W. (1981) *Proc. Natl. Acad. Sci. U.S.A. 78*, 957.

47. Nagarajan, V., Parson, W. W., Davis, D., and Schenck, C. C. (1993) *Biochemistry 32*, 12324.

48. Woodbury, N. W., and Parson, W. W. (1984) *Biochim. Biophys. Acta 767*, 345.

49. Ogrodnik, A., Volk, M., Letterer, R., Feick, R., and Michel-Beyerle, M. E. (1988) *Biochim. Biophys. Acta 936*, 361.

50. Goldstein, R. A., Takiff, L., and Boxer, S. G. (1988) *Biochim. Biophys. Acta 934*, 253.

51. Ogrodnik, A., Keupp, W., Volk, M., Aumeier, G., and Michel-Beyerle, M. E. (1994) *J. Phys. Chem. 98*, 3432.

52. Heller, B. A., Holten, D., and Kirmaier, C. (1996) *Biochemistry 35*, 15418.